Nanopore Identification of Single Nucleotide Mutations in Circulating Tumor DNA by Multiplexed Ligation

Nitza Burck,[a] Tal Gilboa,[a,b,c] Abhilash Gadi,[d] Michelle Patkin Nehrer,[a] Robert J. Schneider,[d,*] and Amit Meller[a,e,*]

BACKGROUND: Circulating tumor DNAs (ctDNAs) are highly promising cancer biomarkers, potentially applicable for noninvasive liquid biopsy and disease monitoring. However, to date, sequencing of ctDNAs has proven to be challenging primarily due to small sample size and high background of fragmented cell-free DNAs (cfDNAs) derived from normal cells in the circulation, specifically in early stage cancer.

METHODS: Solid-state nanopores (ssNPs) have recently emerged as a highly efficient tool for single-DNA sensing and analysis. Herein, we present a rapid nanopore genotyping strategy to enable an amplification-free identification and classification of ctDNA mutations. A biochemical ligation detection assay was used for the creation of specific fluorescently-labelled short DNA reporter molecules. Color conjugation with multiple fluorophores enabled a unique multi-color signature for different mutations, offering multiplexing potency. Single-molecule readout of the fluorescent labels was carried out by electro-optical sensing via solid-state nanopores drilled in titanium oxide membranes.

RESULTS: As proof of concept, we utilized our method to detect the presence of low-quantity ERBB2 F310S and PIK3Ca H1047R breast cancer mutations from both plasmids and xenograft mice blood samples. We demonstrated an ability to distinguish between a wild type and a mutated sample, and between the different mutations in the same sample.

CONCLUSIONS: Our method can potentially enable rapid and low cost ctDNA analysis that completely circumvents PCR amplification and library preparation. This approach will thus meet a currently unmet demand in terms of sensitivity, multiplexing and cost, opening new avenues for early diagnosis of cancer.

Introduction

The ability to identify and quantify genetic variations quickly and accurately in clinical samples has raised intense interest due to its broad medical diagnostic applications. Examples include the classification of antibiotic resistant pathogens (1), controlling the spreading of pandemics (2), and cancer diagnostics especially at the early stages of the disease (3). Circulating tumor DNAs (ctDNAs) are fragments of DNA shed by tumors into the bloodstream. These fragments harbor tumor-specific aberrations, reflecting genetic alterations of the tumors such as point mutations (4), and can be recovered from plasma, serum, and other body fluids (5). Mutations identified from ctDNAs are established biomarkers for early detection of primary and recurrent cancer and their identification can affect treatment outcome. However, the fraction of tumor-originating cfDNA in early stage cancer can be as low as $<0.1\%$, complicating their accurate identification and quantification (6, 7). To become a widespread diagnostic tool, cfDNA detection must overcome the inherent low signal-to-noise ratio (SNR) in the early stages of tumor development, thereby enabling the quantification of an extremely limited copy number of target DNA molecules (8).

Quantification of current ctDNA mutations relies primarily on next generation sequencing (NGS) involving a high degree of polymerase chain reaction (PCR) amplification, but obstacles remain (9, 10). While these technologies have substantially advanced precision medicine forward, they still struggle with providing

[a]Department of Biomedical Engineering, Technion- IIT, Haifa, Israel; [b]Department of Pathology, Brigham and Women's Hospital, Harvard Medical School, Boston, MA, USA; [c]Wyss Institute for Biologically Inspired Engineering, Harvard University, Boston, MA, USA; [d]Department of Microbiology, NYU School of Medicine, New York, NY, USA; [e]Russell Berrie Nanotechnology Institute, Technion- IIT, Haifa, Israel.

*Address correspondence to this author at: NYU School of Medicine, New York, NY 10016, USA. Fax +1 646-501-4541; e-mail Robert.Schneider@nyumc.org. A.M. at Technion-IIT, city Haifa, 3200003, Israel. Fax 972-04-8293202; e-mail ameller@technion.ac.il.

Received September 4, 2020; accepted December 11, 2020.
DOI: 10.1093/clinchem/hvaa328

both sufficient sensitivity and a multiplexing capability beyond a few alleles (11, 12). Those methods involve lengthy sample preparation, including extensive amplification steps which may introduce errors, and require expensive reagents and instrumentation which limit their broad use (13).

Nanopores are portable single-molecule sensing devices that hold great potential for nucleic acid biomarker analysis (14–18). Specifically, solid-state nanopores (ssNPs) can be used to probe low concentrations of DNA molecules from a diluted solution; hence they can be potentially applied for ctDNA quantification (19, 20). In nanopore sensing, a voltage is applied across a thin insulating membrane, typically containing a sub 10 nm size pore, immersed in an electrolyte solution. The ionic current flowing through a single pore is measured using a high bandwidth electrometer. Upon introduction of charged biopolymers to the solution, the local electrical field focuses the sample, and threads individual molecules through the nanopore. Such translocations of biopolymers through the pore induce distinct ion current blockades, with amplitudes and dwell-times that directly correspond to their length, cross section, and charge (21–23).

In recent work, Squires et al. detected insertions and deletions (indels) as well as single nucleotide variations (SNVs) by combining sequence-specific digestions using restriction enzymes, and length classification using ssNPs (24). They showed that probing just a few tens of DNA copies is sufficient to distinguish between 2 SNVs with a confidence level >0.995. This detection method relies on the presence of a recognition site for a restriction enzyme at the mutation site; however, adjusting it to use with clinical samples and multiple targets would be difficult. Thus, a robust complimentary technique for genomic variation detection, which can potentially offer higher multiplexing capabilities is desired (24, 25). The vast majority of nanopore sensing publications to date have used nonclinical DNA molecules, specifically PCR amplicons from plasmids or synthetic DNA; hence the ability to efficiently target specific DNAs directly from clinical samples using nanopore sensor has remained largely unknown.

Ligation-based SNV detection was introduced by Landegren et al. as an assay for detecting the presence of a specific DNA sequence (26). In this technique, two ligation probes are hybridized to denatured DNA template such that the 5' end of the first probe is adjacent to the 3' end of the second probe. DNA ligase is then introduced, and will catalyze the formation of a phosphodiester bond between the two probes only if the nucleotides at the junction are correctly base paired to the template. Hence, by designing oligo pairs which meet at the mutation site, this method can distinguish between normal and mutated DNA, even if they differ by just a single nucleotide (27, 28). This method was proven to be highly accurate and specific, and an effective tool for SNV detection mainly by fluorescence resonance energy transfer (FRET) measurements in which each of the two ligation probes is labeled with a fluorescence dye. However, it lacks sufficient multiplexing ability to allow probing many genetic variations simultaneously (29).

To enable multiplexed, specific, and sensitive mutations detection using ssNPs, we have developed an assay in which unique genetic variations are converted to a molecular form via sequence specific ligation, that could be observed using orthogonal electro-optical sensing (29–32). In our technique, an electrical voltage is used to focus the biomolecules to the ssNP, and to control their translocation speed. On the other hand, optical information is obtained from the fluorescence signals emitted by the molecules during their passage through the pore. Here, we present a proof-of-principle of our ability to use this molecular typing technique for direct, nanopore-based, cancer genotyping.

Materials and Methods

To demonstrate our assay's capabilities towards the goal of cancer amplification-free genotyping, we created a breast cancer model. A library of ligation detection probes was designed to recognize chosen breast cancer mutations. Each mutation detection 'set' was comprised of a biotinylated probe for separation using streptavidin-coated beads and a 'tags' probe labelled with its own unique fluorescent color marker. Each of these probes had a different combination and number of fluorophores that was read using the nanopore sensor, and uniquely identified the presence of a mutation in the sample. Notably, the coincident recording of the independent electrical and optical signals reduced the chances of false positive results.

PROBE DESIGN AND LABELLING

Ligation primers were designed to match the sequence of the gene of interest and to meet at the mutation point (Supplemental Table 1). Each set of detection probes was comprised of two primers: First, a probe containing a phosphate on the 3' end to allow the ligation reaction and a 5' biotin for separation. Second, a probe labelled by a unique fluorescent sequence. This primer had a poly-dT tail to which fluorophores were attached, spaced 20 bp from each other to minimize FRET (33). Polyacrylamide gel electrophoresis (PAGE) purified primers (IDT) included an amine chemical modification to the DNA backbone at the labelling sites. The amine group covalently binds to an NHS ester on the fluorophore in slightly alkaline conditions (pH 7.2 to 9) to yield stable amide bonds. Fluorophores used were DyLight 550-NHS ester or DyLight 650-NHS ester,

and labelling was carried overnight, followed by ethanol precipitation purification to remove the unconjugated dyes. Labelling efficiency was estimated by UV-VIS absorption (Agilent Technologies Cary60) as provided in the Supporting Information (Supplemental Fig. 1).

LIGATION DETECTION ASSAY

Taq ligase, a highly thermostable enzyme, was used to catalyze the formation of a phosphodiester bond between juxtaposed 5' phosphate and 3' hydroxyl termini of 2 adjacent oligonucleotides when they are hybridized to a complementary target DNA. Its thermo-stability is important for the ligation assay since it involves denaturation of the DNA by heating it to 94 °C. For the ligation process, the template DNA (100 ng of 632 bp long template DNA WT or mutated in each reaction) being analyzed for the presence of mutations was mixed with the probes (template to probes ratio was 100:1), ligase and the Ligation buffer (20 mmol/L Tris-HCl, 100 mmol/L potassium acetate, 1 mmol/L magnesium acetate, 1 mmol/L NAD1, 10 mmol/L DTT, 0.1% Triton X-100, pH 7.6). These conditions were selected after an optimization step (see Supplemental Information section 5). Next, the mixture was heated to 94 °C to denature the DNA and then the temperature was lowered to 52 °C to allow the ligation reaction. The temperature was cycled 30 times between these 2 temperatures until terminated by cooling.

ELECTRO-OPTICAL SENSING

For the synchronous optical and electrical measurements, a nanopore chip was glued to a plastic cell and mounted on a closed-loop XYZ piezo nanopositioner (Physik Instrumente, P-561.3), with the backside facing the high-NA objective (Zeiss Plan Apochromat 63x/1.15). Two lasers with center wavelengths at 561 nm and 640 nm (iFlex-Viper, QIOptiq) were combined and coupled to the system via a single-mode, polarization preserving, optical fiber. The laser emission beams were cleaned using the proper bandpass filters (Chroma), and their intensities were controlled using a variable natural density filter wheel (Thorlabs). A custom-made telescope was used to expand the laser beam to fully cover the back aperture of the objective, hence creating a diffraction-limited excitation spot. The emitted light was collected by the same objective, followed by the appropriate long pass and notch filters (Chroma) and focused using a single 20 cm focal length lens. The emitted light was focused to either a charge coupled device (CCD) camera used for initial alignment of the chip window, or a 50 µm pinhole (Thorlabs) in confocal mode. Light passing through the pinhole was collimated by a 10 cm lens and split using a dichroic mirror (Semrock) with center wavelengths of $\lambda = 650$ nm. The split light was focused onto 2 avalanche photodiodes (APD)s (Perkin Elmer SPCM- AQR-14) using 2.5 cm focal length achromatic doublet lenses. All lenses were obtained from Thorlabs. The ion current through the nanopore was synchronously measured by 2 Ag/AgCl electrodes connected to an Axon Axopatch 200B patch-clamp filtered at 10 KHz. The sample cell was placed in a darkened Faraday cage to prevent external electromagnetic noise. We used National Instruments NI-6602 for photon counting (sampled at 500 KHz) and a NI-6154 DAQ for the electrical signal acquisition (filtered sampled at 125 KHz). The 2 cards were synchronized via a common hardware connection. A custom LabVIEW (National Instrument) program was developed to fully control the system. See the Supplemental Information section 6 for detailed description of the signal acquisition and analysis steps.

Results

ELECTRO-OPTICAL SENSING OF SINGLE NUCLEOTIDE MUTATIONS IN NANOPORES

The general workflow of our method for rapid, amplification-free, nanopore screening of circulating tumor biomarkers is illustrated in Fig. 1A. DNA samples, harboring or lacking specific DNA target sequences were used as a template for sequence-specific ligation biochemistry resulting in single strand DNA (ssDNA) reporter fragments that were detected in the nanopore sensor. This was achieved by a library containing multiple pairs of ssDNA ligation probes, named the "tags probe" and "separation probe," designed to target each genomic variation. The tags probes contained 3 fluorescent moieties to permit single-molecule counting using the nanopore biosensor. Each fluorophore combination represented a specific mutation which could be uniquely identified. The selection probes were biotinylated to facilitate the downstream separation process. The two probes were ligated only when they were correctly based paired to the template (27, 28). Thus, the ligation occurred only in the presence of the target SNV. Following ligation, streptavidin-coated magnetic beads were used for separation of our reporter fragments (see Supplemental Information section 7). Finally, the reporter fragments were read by the electro-optical nanopore device (30) providing direct counting of each of the mutations in each sample (see Methods and Supplemental Information section 8).

Here we used nanopores in the range of $2-3$ nm diameter drilled by dielectric breakdown (see Supplemental Information section 9) in ultra-thin membranes of titanium dioxide (TiO_2) that we deposited in house using an Atomic Layer Deposition (ALD) process (see Supplemental Information section 10). These freely

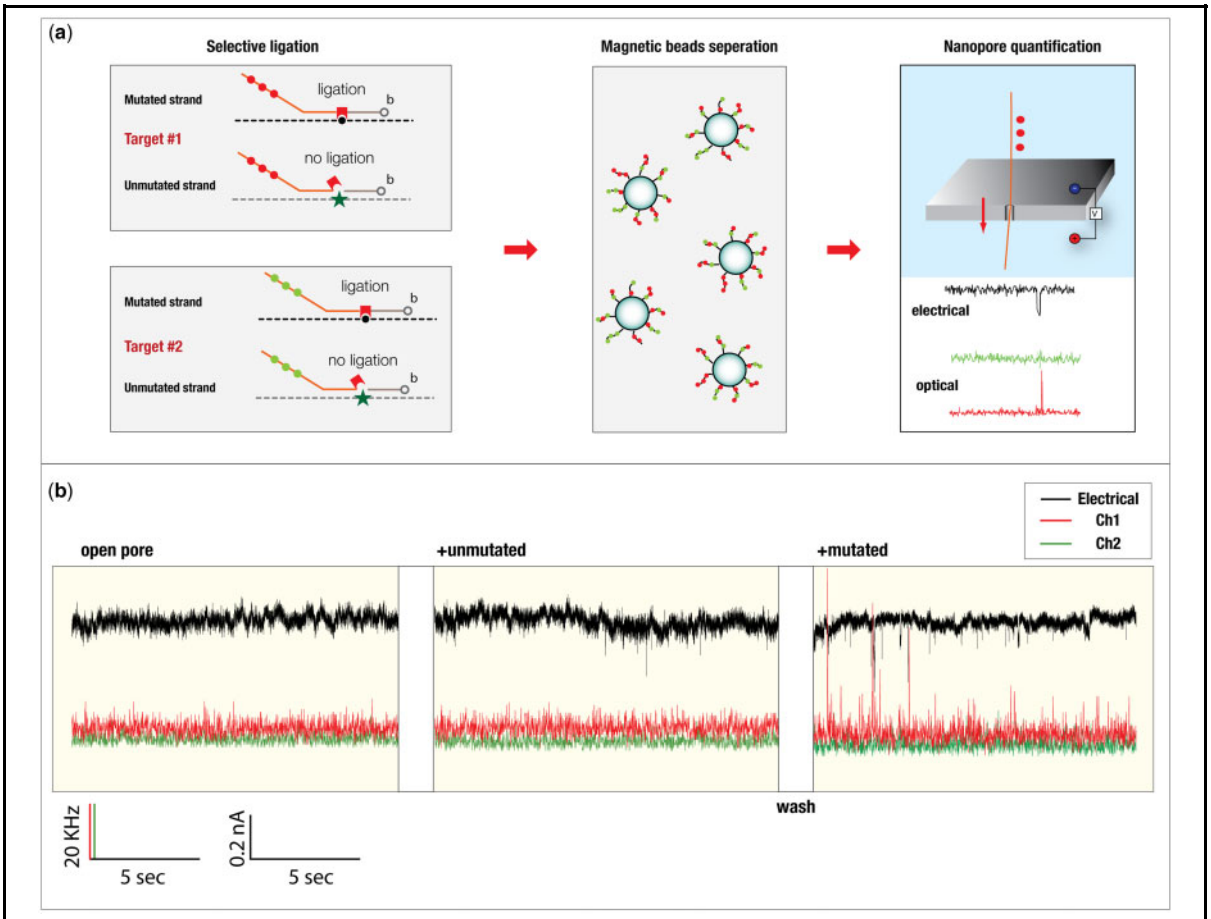

Fig. 1. A schematic description of the ligation-nanopore detection method for single molecule DNA mutation classification. (A) Sequence-specific ligation is carried out for mutation identification, creating single stranded DNA reporting fragments only if the variations are present in the DNA sequence. Each reporting fragment is labelled with a unique identifier fluorescent tag. The fragments are then captured on Streptavidin-coated magnetic beads for purification, separating only the products of the ligation reaction. The reporting fragments are then released from the beads using heat, and finally, analyzed one by one using electro-optical nanopore biosensors indicating whether specific mutations are present in the sample. (B) Electro-optical traces for mutation identification. The nanopore ion current and the fluorescence emissions are interrogated simultaneously. From left to right: before adding any sample, after addition of unmutated sample, and after addition of the mutated sample. The sample chamber was washed in between samples. As the unmutated sample is analyzed, electrical spikes are observed due to the presence of separation probes in the sample. But when the mutated sample is introduced, simultaneous downward spike in the ion current and upward photon bursts are apparent. Electrical signals from free separation probes are still seen, as well as some optical spikes from molecules entering the confocal spot but not the pore. These are rejected later in the signal analysis process.

standing membranes were 20 nm thick and previously found to exhibit an extremely low optical background, which was critical for single-molecule optical sensing (31). Figure 1B shows a typical sensing process using our system. The current trace (gray line) and the optical signals in the two detection channels (blue and red lines) were recorded before any sample was added, after the WT sample was introduced, and finally after it was replaced with the mutated sample. First, we could assess the systems noise for both acquired signals prior to adding any analyte. Next, after adding the product from the ligation reaction with WT template into the *cis* chamber, electrical current drops were observed, indicating translocation events of the unlabeled single stranded separation probe. No changes were detected in the optical signal. Nonetheless, when replacing the sample with

a ligation product from a mutated sample, drops in electrical current, as well as spikes in photon counts were clearly observed. Thus, these data indicated that both unlabeled (separation probes) and labelled (ligation products) strands were entering both the pore and the confocal illumination spot of our system (Supplemental Information section 11).

VALIDATION OF THE LIGATION DETECTION SCHEME

We evaluated our method by synthesizing plasmids containing the sequences of the well-characterized breast cancer mutations ERBBS S310F and PIK3Ca H1047R. These were model genes in which specific mutations are considered actionable and their identification may be used to affect patient's treatment (36, 37). First, we synthesized and linked multiple 15 bp DNA segments harboring the unmutated or mutated sequences and inserted them into an RFP-selectable retrovirus (Fig. 2A). These plasmids provided a target for assay development and lacked the irrelevant biological activity.

We designed two sets of probes that could identify the presence of both mutations (Supplemental Information section 3). Sequence specific ligation detection assay was performed both using the unmutated and mutated sequences, exercising the library containing our fluorescently labelled detection probes:three DyLigt650 dyes or three Dylight550 dyes indicating the presence of either ERBB2 S310F mutation or PIK3Ca H1047R mutation, respectively (Supplemental Information section 4). The ligation reaction yield was found to be 72.2% for ERBB2 S310F and 55% for PIK3Ca H1047R, which means that 15.8 and 20.7 reporting molecules were retrospectively created for each template molecule in the reaction mix (Supplemental Information section 5.3). Following ligation, streptavidin-coated bead separation was used to wash unligated labelled oligos to avoid false positive results (Supplemental Information section 7).

To validate our biochemical assay in bulk we ran the ligation products on a 15% PAGE. The gels were scanned using 2 color laser scanner (Bio-Rad, Pharos FX) and subsequently stained with SYBR Gold in order to highlight the unlabeled DNA bands. The overlay of these images is shown in Fig. 2B and C. We noted that ligation products were specific as band appeared only for the mutated samples for both mutations (lanes #3 in both gels), whereas they were not formed with the unmutated templates (lanes #4–#6). Moreover, lanes #2 in both gels showed that the probe oligos could effectively capture the target ligated products as the flow-through did not contain visible traces of the ligated product. These results confirmed that our ligation assay, with the labelled probes and bead separation steps, could be used to specifically identify the presence of SNVs in a DNA sample. For both samples, the short biotinylated separation probe was released in large quantity from the magnetic beads. However, since they were unlabelled, they were not expected to interfere with downstream nanopore analysis.

After validating our ligation assay in bulk, we analyzed the two ligation products using our ssNPs. Moving to the sensitive single molecule counting approach required dilution of samples by >2000 fold, underlying its potential for detecting SNVs in dilute clinical samples. In Fig. 2D, our ability to discriminate between two mutations is shown. Analysis of the synchronized recording of the electrical and optical traces (concatenated to preserve space) in two colors, distinct events representing the identity of their source can be observed . Each electrical DNA translocation event (gray curve) is accompanied by a unique burst of photons in either the "green" (DyLight550) or "red" (DyLight650) detectors. This concept can be expanded for multiplexed detection of more mutations by using additional colors, longer sequences, different color compositions, or even by using other labelling methods (32).

NANOPORE MUTATION DETECTION FROM BLOOD SAMPLES

We further evaluated the applicability of our method for the detection of mutations directly from blood. When blood sample volumes are restricted, using conventional methods involving amplification has proven to be extremely challenging. To this end, xenograft breast cancer mouse models were created using two types of mouse tumor populations corresponding to the unmutated or mutant gene sequences, differing from each other only by the presence of the single nucleotide mutation sequence (Fig. 3A).

The synthesized plasmids, used for assay validation, were propagated, and used to transform the DNA sequences into the highly malignant breast cancer cell line MDA-MB-231 breast cancer cells at low copy number (Fig. 3B, Supplemental Information section 1). MDA-MB-The cells were transduced with vectors containing either the unmutated or mutant sequences (left and right columns in Fig. 4, respectively), which were stably transformed and identified by Red Fluorescent Protein (RFP), as shown in Fig. 4c. RFP expressing cells were isolated by FACS and shown to be stably transformed to similar extents. The advantage of this strategy, as opposed to comparing tumor growing mouse blood with healthy mouse, was that in our strategy the two mouse models were identically treated, providing more reliable physiological baseline. Approximately $5{\cdot}10^6$ cells (parental or engineered) were then injected into the flank of NOD/SCID/γ mice immune-deficient mice (8 mice per group). Tumors developed within two weeks and began to metastasize

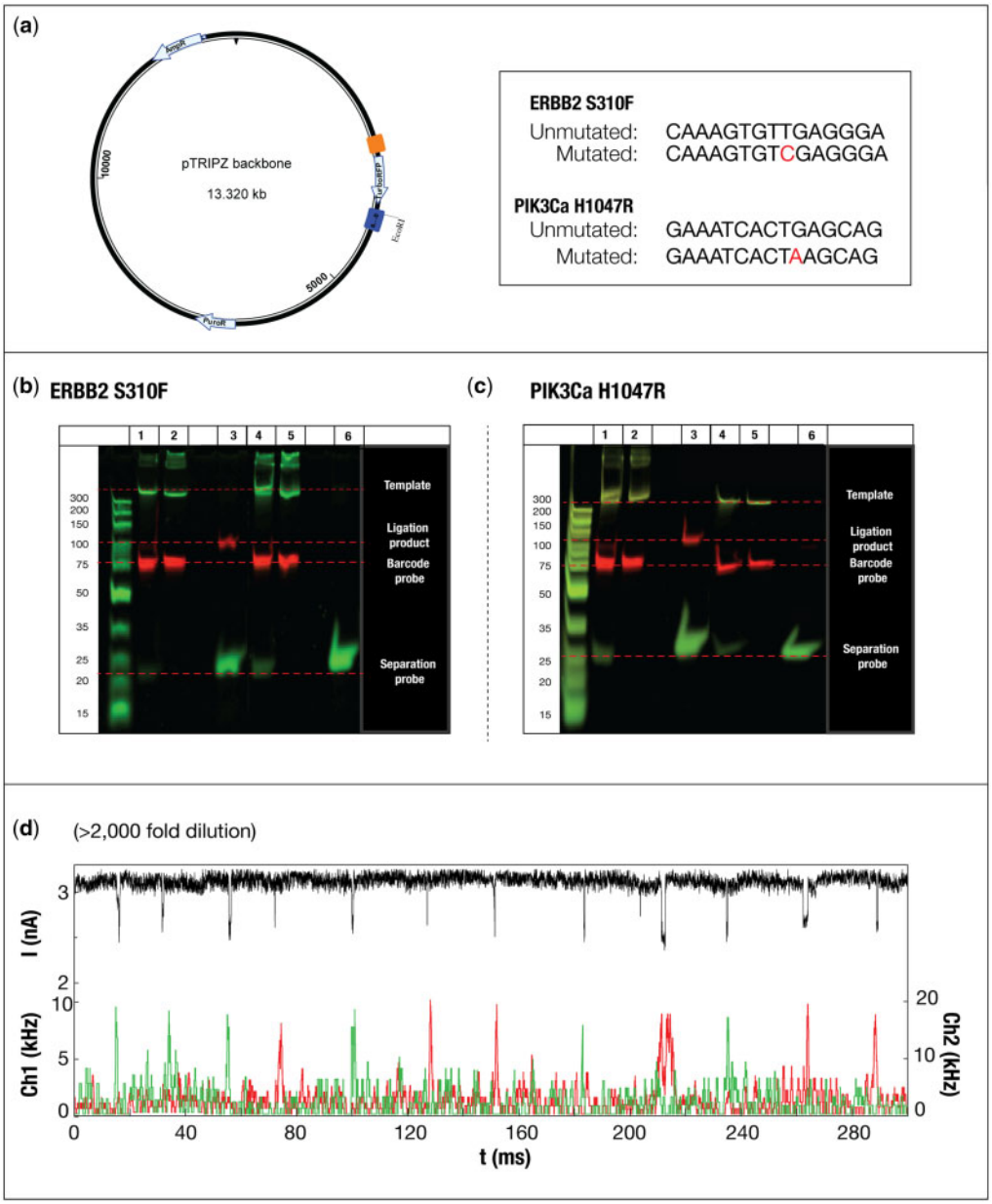

Fig. 2. Design and in vitro validation of DNA vectors containing target oncogenes sequences. (A) Target DNA sequences for the ERBB2 S310F and PIK3Ca H1047R mutations (shown in the table) inserted into a pTRIPZ vector. The plasmid was used for validation of ligation-based mutation identification scheme performed in bulk. (B) PAGE analysis is shown for ERBB2 S310F mutation, and (C) for PIK3Ca H1047R mutation. Green bands are of DNA stained with SYBR gold, while red bands are of fluorescently labelled DNA. Lane 1 is the ligation mix composed of the template DNA containing the mutation, the two detection probes and the ligation product created in the process. Lane 2 is the beads flow-through; any nucleic acids that did not bind to the streptavidin coated beads (i.e., the template and biotinylated probe). Lane 3 is the released purified product after bead separation (i.e., the reporting DNA fragment and unlabeled separation probe). Lanes 4–6 represent the same for the control sample (unmutated template). Notably, no ligation reporting fragment was created in this case. (D) Synchronous electrical (gray) and optical signals (green and red) obtained from ssDNA ligation reporting fragments during translocation through a ~2 nm solid-state nanopore. Detection of the ligation product labelled with 3 DyLight550 dyes indicates that the analyzed samples harbors the PIK3Ca H1047R mutation, while obtaining a signal from the red channel, meaning a ligation product labelled with 3 DyLight650 dyes, indicated that the analyzed sample harbors the ERBB2 S310F mutation.

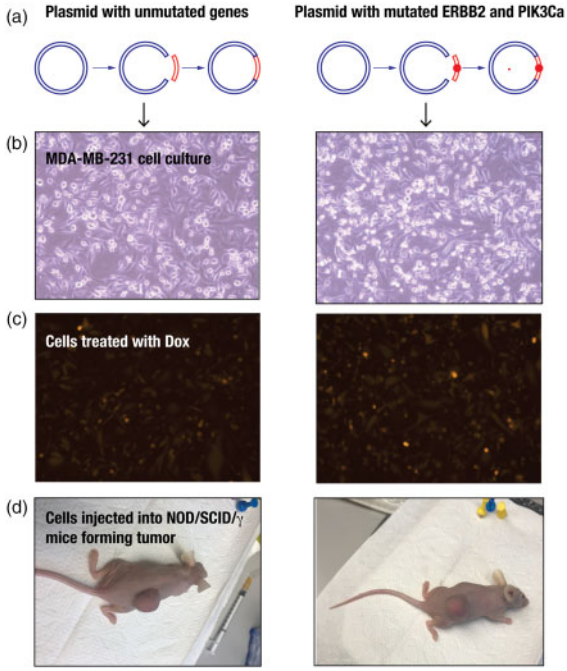

Fig. 3. Construction of a xenograft mouse model for assay validation. (A) DNA plasmids containing the unmutated or mutated sequences were introduced into MB-231 breast cancer cell line (B), and cells were allowed to proliferate. Puromycin-positive selection was performed as shown by using doxycycline (C), and the newly engineered cells were injected into nude mice and left to grow, metastasize, and release DNA into the bloodstream (D). Ill mice were physically identical, differing only in the presence of the mutated target sequence in the injected breast cancer cells. After 3–5 weeks, mice were bled, and DNA was collected and purified from their plasma. The collected cfDNA was isolated from the blood using the Invitrogen MagMax cfDNA isolation kit.

within four weeks. Notably, both the control mice (left hand column), harboring the unmutated plasmid and the mice harboring the mutated plasmid (right hand column) reacted similarly to the injection of the MDA-MB-231 cells and developed visually indistinguishable phenotypes (Fig. 3D). Therefore, statistically identical releases of cfDNA molecules were expected to be shed into the mouse bloodstreams, enabling a clear comparison between the two (36).

At 5–6 weeks mice were anesthetized with isoflurane, and exsanguinated by aortic cardiac puncture, collecting on average 1.5 mL of blood. cfDNA was isolated from the blood using the Invitrogen MagMax cfDNA isolation kit (Supplemental Information section 2). The extracted cfDNA was then subjected to our ligation detection assay with the library probe designed to detect the ERBB2 S310F and PIK3Ca mutations, as explained in Fig. 1. After bead separation, samples from both the unmutated and mutated blood samples were analyzed by our ssNPs system. Even though our samples were extracted from just 1.5 mL of total blood, after subjecting it to the ligation and bead purification steps, the optical signals originating from the unmutated sample produced only background level of fluorescence (Fig. 4A), whereas the mutated sample exhibited clearly distinguishable optical spikes both in the red and green channels corresponding to passages of the target DNA molecules through the nanopore (Fig. 4B). Both samples produced electrical translocation events (Supplemental Information section 11), confirming that DNA molecules were equally present.

The left panels in Fig. 4 present about 50 s of continuous recording of the samples. In principle, these data are sufficient to distinguish among the unmutated and mutated samples with reasonable confidence. To further solidify the results, we collected the signals for an extended period of time sufficient to obtain hundreds of optical events and clearly count the number of mutated DNA copies, as shown in the events heat map (Fig. 4, right-hand panels). These data show the ability to resolve the two mutations in the sample solely according to the rise in photon count during their translocation events. The signal threshold level used to define the

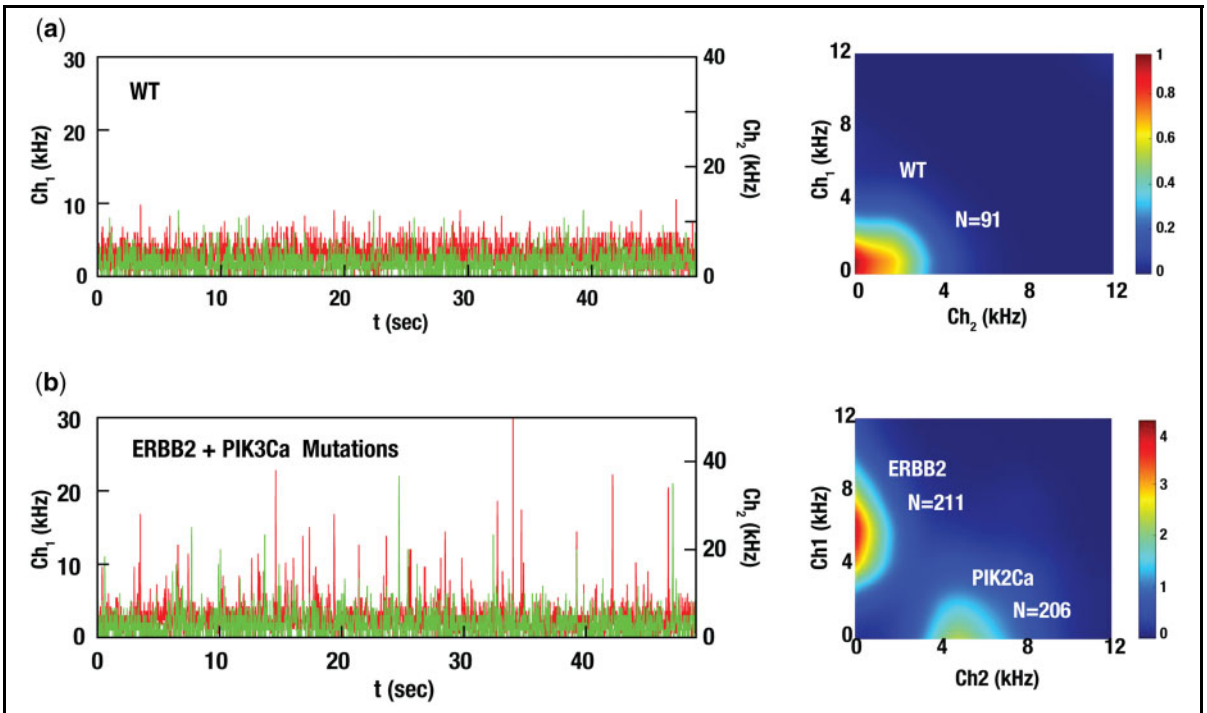

Fig. 4. Analysis of the single molecule ctDNA mutation identification from the xenograft mice blood. Two samples are compared: (A) blood samples from the mice treated with MB-231 breast cancer harboring the WT plasmid; (B) blood samples from the mice treated with MB-231 breast cancer harboring the mutated plasmid. In both cases, the blood samples are subjected to the ligation assay (Fig. 1) and analyzed optically with solid-state nanopores using two colors simultaneously. Representative 50 s time traces are shown. The unmutated sample (A) does not exhibit photon pulses beyond the background noise, but the mutated sample (B) shows clear red and green photons spikes, corresponding to the two mutations ERBB2 S310F and PIK3Ca H1047R, respectively. Electrical spikes are present in both cases (not shown). The optical scatter plot of green channel versus red channel (right panels) shows no distinct signal for the unmutated sample as expected, but presents two distinct populations, allowing quantitative differentiation between the two DNA mutations: ERBB2 S310F and PIK3Ca H1047R directly from the mouse blood sample.

optical bursts on the WT data was used to evaluate the false positive ratio (Supplemental Information section 12) and the specificity of our assay, determined to be ∼96.6%.

Discussion

We present a new method for rapid detection and quantification of therapy-resistant and actionable genetic alterations from clinical samples (blood). SsNPs are considered to be highly-sensitive single-molecule biosensors because charged molecules, such as DNA, are actively funneled to the nanopore by long-range electrical forces (19). To date, however, ssNPs have primarily been applied for sensing synthetic, purified, or highly-amplified biomolecule products. To adapt these biosensors for complex nucleic acids biomarker quantification, such as circulating tumor DNAs, present at very low abundance, we developed and demonstrated a ligation-based biochemical assay. Taking advantage of the high sensitivity and multiplexing capability of the parallel electro-optical sensing in nanopores, we performed direct nanopore analysis of circulating DNAs from blood samples.

To validate the assay, we developed xenotransplant mouse tumor models for human breast cancers expressing either unmutated control or specific mutated forms of driver-mutated genes as a source for sera. Importantly, both the control mice and the mutated genes mice were equally treated and developed similar physiological states of breast cancer. The extracted DNA was processed using our ligation biochemical assay, and the results were analyzed by our electro-optical nanopore sensors, thereby demonstrating the method's ability to specifically genotype ERBB2 S310F and PIK3CA H1047R mutations in blood from a mouse model.

The TiO_2-based nanopore devices exhibited negligible photoluminescence and improved SNR (31), resulting in high specificity in classifying a mutated molecule. Future work will be focused on exploring metallic coatings (37) to further suppress optical fluorescence background to improve the detection accuracy. Here, we measured total fluorescence arising from each molecule, which can be used to quantify the number of fluorophores labelling composition (38), uniquely identifying each mutation. This approach can be further expanded to increase multiplexing capabilities by using plasmonic nanopores and molecular beacons (31, 33), paving the way for novel early phase cancer screening.

Nonstandard Abbreviations: ALD, atomic layer deposition; APD, avalanche photodiodes; CBD, controlled dielectric breakdown; cfDNA, cell-free DNA; ctDNA, circulating tumor DNA; FRET, fluorescence resonance energy transfer; NGS, next generation sequencing; PAGE, polyacrylamide gel electrophoresis; PCR, polymerase chain reaction; SNR, signal-to-noise ration; SNV, single nucleotide variation; ssDNA, single-stranded DNA; ssNP, solid-state nanopore

Human Genes: *ERBB2*, erb-b2 receptor tyrosine kinase; *PIK3CA*, phosphatidylinositol-4,5-bisphosphate 3-kinase catalytic subunit alpha

Author Contributions: *All authors confirmed they have contributed to the intellectual content of this paper and have met the following 4 requirements: (a) significant contributions to the conception and design, acquisition of data, or analysis and interpretation of data; (b) drafting or revising the article for intellectual content; (c) final approval of the published article; and (d) agreement to be accountable for all aspects of the article thus ensuring that questions related to the accuracy or integrity of any part of the article are appropriately investigated and resolved.*

R.J. Schneider, financial support, provision of study material or patients; A. Meller, financial support.

Authors' Disclosures or Potential Conflicts of Interest: *Upon manuscript submission, all authors completed the author disclosure form. Disclosures and/or potential conflicts of interest:*

Employment or Leadership: None declared.
Consultant or Advisory Role: None declared.
Stock Ownership: None declared.
Honoraria: None declared.
Research Funding: Funding from the European Research Council (ERC) under the European Union's Horizon 2020 research and innovation programme grant agreement No. 833399 (NanoProt-ID)and support from the ISF award 3485/19.
Expert Testimony: None declared.
Patents: None declared.

Role of Sponsor: The funding organizations played no role in the design of study, choice of enrolled patients, review and interpretation of data, preparation of manuscript, or final approval of manuscript.

References

1. Fluit AC, Visser MR, Schmitz FJ. Molecular detection of antimicrobial resistance. Clin Microbiol Rev 2001;14:836–71.
2. Pan C, Cheung B, Tan S, Li C, Li N, Liu S, Jiang S. Genomic signature and mutation trend analysis of pandemic (H1N1) 2009 Influenza A virus. PLoS One 2010;5:e9549.
3. Morash M, Mitchell H, Beltran H, Elemento O, Pathak J. The role of next-generation sequencing in precision medicine: a review of outcomes in oncology. J Pers Med 2018;8:30.
4. Talmadge JE, Fidler IJ. The biology of cancer metastasis: historical perspective. Cancer Res 2010;70:5649–69.
5. Fan HC, Blumenfeld YJ, Chitkara U, Hudgins L, Quake SR. Analysis of the size distributions of fetal and maternal cell-free DNA by paired-end sequencing. Clin Chem 2010;56:1279–86.
6. Haber DA, Velculescu VE. Blood-based analyses of cancer: circulating tumor cells and circulating tumor DNA. Cancer Discov 2014;4:650–61.
7. Saliou A, Bidard F-C, Lantz O, Stern M-H, Vincent-Salomon A, Proudhon C, Pierga J-Y. Circulating tumor DNA for triple-negative breast cancer diagnosis and treatment decisions. Expert Rev Mol Diagn 2016;16:39–50.
8. Schubert SM, Arendt LM, Zhou W, Baig S, Walter SR, Buchsbaum RJ, et al. Ultra-sensitive protein detection via single molecule arrays towards early stage cancer monitoring. Sci Rep 2015;5:11034.
9. Cohen SJ, Punt CJA, Iannotti N, Saidman BH, Sabbath KD, Gabrail NY, et al. Relationship of circulating tumor cells to tumor response, progression-free survival, and overall survival in patients with metastatic colorectal cancer. J Clin Oncol 2008;26:3213–21.
10. Dawson S, Tsui DWY, Murtaza M, Biggs H, Rueda OM, Chin S, et al. Analysis of circulating tumor DNA to monitor metastatic breast cancer. N Engl J Med 2013;368:1199–209.
11. Perkins G, Yap TA, Pope L, Cassidy AM, Dukes JP, Riisnaes R, et al. Multi-purpose utility of circulating plasma DNA testing in patients with advanced cancers. PLoS One 2012;7:e47020.
12. Murtaza M, Dawson S, Tsui DWY, Gale D, Forshew T, Piskorz AM, et al. Non-invasive analysis of acquired resistance to cancer therapy by sequencing of plasma DNA. Nature 2013;497:108–12.
13. Bronkhorst AJ, Ungerer V, Holdenrieder S. The emerging role of cell-free DNA as a molecular marker for cancer management. Biomol Detect Quantif 2019;17:100087.
14. Tian K, Decker K, Aksimentiev A, Gu L. Interference-free detection of genetic biomarkers using synthetic dipole-facilitated nanopore dielectrophoresis. ACS Nano 2017;11:1204–13.
15. Tian K, Chen X, Luan B, Singh P, Yang Z, Gates KS, et al. Single locked nucleic acid-enhanced nanopore genetic discrimination of pathogenic serotypes and cancer driver mutations. ACS Nano 2018;12:4194–205.
16. Bell NAW, Keyser UF. Digitally encoded DNA nanostructures for multiplexed, single-molecule protein sensing with nanopores. Nat Nanotech 2016;11:645–51.
17. Gu LQ, Gates KS, Wang MX, Li G. What is the potential of nanolock– and nanocross–nanopore technology in cancer diagnosis? Expert Rev Mol Diagn 2018;18:113–7.
18. Ding T, Yang J, Pan V, Zhao N, Lu Z, Ke Y, Zhang C. DNA nanotechnology assisted nanopore-based analysis. Nucleic Acids Res 2020;48:2791–806.
19. Wanunu M, Morrison W, Rabin Y, Grosberg AY, Meller A. Electrostatic focusing of unlabelled DNA into nanoscale pores using a salt gradient. Nat Nanotech 2010;5:160–5.
20. Wang Y, Tian K, Shi R, Gu A, Pennella M, Alberts L, et al. Nanolock-nanopore facilitated digital diagnostics of cancer driver mutation in tumor tissue. ACS Sens 2017;2:975–81.
21. Atas E, Singer A, Meller A. DNA sequencing and barcoding using solid-state nanopores. Electrophoresis 2012;33:3437–47.
22. Meller A, Nivon L, Branton D. Voltage-driven DNA translocations through a nanopore. Phys Rev Lett 2001;86:3435–8.
23. Meller A, Nivon L, Brandin E, Golovchenko J, Branton D. Rapid nanopore discrimination between single polynucleotide molecules. Proc Natl Acad Sci USA 2000;97:1079–84.
24. Squires AH, Atas E, Meller A. Genomic pathogen typing using solid-state nanopores. PLoS One 2015;10:e0142944.
25. Weckman NE, Ermann N, Gutierrez R, Chen K, Graham J, Tivony R, et al. Multiplexed DNA identification using site specific dCas9 barcodes and nanopore sensing. ACS Sens 2019;4:2065–72.
26. Landegren U, Kaiser R, Sanders J, Hood L. A ligase-mediated gene detection technique. Science 1988;241:1077–80.
27. Kaur M, Zhang Y, Liu W-H, Tetradis S, Price BD, Makrigiorgos GM. Ligation of a primer at a mutation: a method to detect low level mutations in DNA. Mutagenesis 2002;17:365–74.
28. Heidari Sharafdarkolaei S, Motovali-Bashi M, Gill P. Fluorescent detection of point mutation via ligase reaction assisted by quantum dots and magnetic nanoparticle-based probes. RSC Adv 2017;7:25665–72.
29. McNally B, Singer A, Yu Z, Sun Y, Weng Z, Meller A. Optical recognition of converted DNA nucleotides for single-molecule DNA sequencing using nanopore arrays. Nano Lett 2010;10:2237–44.
30. Gilboa T, Meller A. Optical sensing and analyte manipulation in solid-state nanopores. Analyst 2015;140:4733–47.

31. Wang R, Gilboa T, Song J, Huttner D, Grinstaff MW, Meller A. Single-molecule discrimination of labeled DNAs and polypeptides using photoluminescent-free TiO_2 nanopores. ACS Nano 2018;12:11648–56.

32. Assad ON, Fiori N, Di Squires AH, Meller A. Two color DNA barcode detection in photoluminescence suppressed silicon nitride nanopores. Nano Lett 2015;15:745–52.

33. Murphy MC, Rasnik I, Cheng W, Lohman TM, Ha T. Probing single-stranded DNA conformational flexibility using fluorescence spectroscopy. Biophys J 2004;86:2530–7.

34. Greulich H, Kaplan B, Mertins P, Chen T-H, Tanaka KE, Yun C-H, et al. Functional analysis of receptor tyrosine kinase mutations in lung cancer identifies oncogenic extracellular domain mutations of ERBB2. Proc Natl Acad Sci U S A 2012;109:14476–81.

35. Shimoi T, Hamada A, Yamagishi M, Hirai M, Yoshida M, Nishikawa T, et al. PIK3CA mutation profiling in patients with breast cancer, using a highly sensitive detection system. Cancer Sci 2018;109:2558–66.

36. Gorges TM, Schiller J, Schmitz A, Schuetzmann D, Schatz C, Zollner TM, et al. Cancer therapy monitoring in xenografts by quantitative analysis of circulating tumor DNA. Biomarkers 2012;17:498–506.

37. Assad ON, Gilboa T, Spitzberg J, Juhasz M, Weinhold E, Meller A. Light-enhancing plasmonic-nanopore biosensor for superior single-molecule detection. Adv Mater 2017;29:1605442.

38. Gilboa T, Torfstein C, Juhasz M, Grunwald A, Ebenstein Y, Weinhold E, Meller A. Single-molecule DNA methylation quantification using electro-optical sensing in solid-state nanopores. ACS Nano 2016;10:8861–70.